Cellular and Molecular Life Sciences (2020) 77:3215–3229
https://doi.org/10.1007/s00018-019-03343-7

ORIGINAL ARTICLE

miR-182-5p is an evolutionarily conserved Tbx5 effector that impacts cardiac development and electrical activity in zebrafish

Elena Guzzolino[1,2] · Mario Pellegrino[3] · Neha Ahuja[4] · Deborah Garrity[4] · Romina D'Aurizio[5] · Marco Groth[6] · Mario Baumgart[6] · Cathy J. Hatcher[7] · Alberto Mercatanti[1] · Monica Evangelista[1] · Chiara Ippolito[8] · Elisabetta Tognoni[3] · Ryuichi Fukuda[9] · Vincenzo Lionetti[2,10] · Marco Pellegrini[5] · Federico Cremisi[11] · Letizia Pitto[1]

Received: 11 April 2019 / Accepted: 14 October 2019 / Published online: 4 November 2019
© Springer Nature Switzerland AG 2019

Abstract

To dissect the *TBX5* regulatory circuit, we focused on microRNAs (miRNAs) that collectively contribute to make TBX5 a pivotal cardiac regulator. We profiled miRNAs in hearts isolated from wild-type, *CRE, Tbx5*$^{lox/+}$ *and Tbx5*$^{del/+}$ mice using a Next Generation Sequencing (NGS) approach. TBX5 deficiency in cardiomyocytes increased the expression of the miR-183 cluster family that is controlled by Kruppel-like factor 4, a transcription factor repressed by TBX5. MiR-182-5p, the most highly expressed miRNA of this family, was functionally analyzed in zebrafish. Transient overexpression of miR-182-5p affected heart morphology, calcium handling and the onset of arrhythmias as detected by ECG tracings. Accordingly, several calcium channel proteins identified as putative miR-182-5p targets were downregulated in miR-182-5p overexpressing hearts. In stable zebrafish transgenic lines, we demonstrated that selective miRNA-182-5p upregulation contributes to arrhythmias. Moreover, cardiac-specific down-regulation of miR-182-5p rescued cardiac defects in a zebrafish model of Holt–Oram syndrome. In conclusion, miR-182-5p exerts an evolutionarily conserved role as a TBX5 effector in the onset of cardiac propensity for arrhythmia, and constitutes a relevant target for mediating the relationship between *TBX5*, arrhythmia and heart development.

Keywords microRNAs · Holt–Oram syndrome · Zebrafish · Cardiac development

Introduction

The T-box transcription factor 5 (TBX5) is an essential transcription factor (TF) for heart development [1]. *TBX5* mutations cause Holt–Oram syndrome (HOS), an autosomal dominant disorder characterized by severe upper limb and

Electronic supplementary material The online version of this article (https://doi.org/10.1007/s00018-019-03343-7) contains supplementary material, which is available to authorized users.

✉ Letizia Pitto
l.pitto@ifc.cnr.it

1 Institute of Clinical Physiology, National Research Council, IFC via Moruzzi 1, 56124 Pisa, Italy

2 Institute of Life Sciences, Scuola Superiore Sant'Anna, Pisa, Italy

3 National Institute of Optics, CNR, Pisa, Italy

4 Department of Biology, Colorado State University (CSU), Fort Collins, CO, USA

5 Institute of Informatics and Telematics, CNR, Pisa, Italy

6 The Leibniz Institute on Aging, Fritz Lipmann Institute (FLI), Jena, Germany

7 Department of Bio-Medical Sciences, Philadelphia College of Osteopathic Medicine, Philadelphia, PA, USA

8 Department of Clinical and Experimental Medicine, University of Pisa, 56126 Pisa, Italy

9 Department of Developmental Genetics, Max Planck Institute for Heart and Lung Research, Bad Nauheim, Germany

10 UOS Anesthesiology, Fondazione Toscana "G.Monasterio", Pisa, Italy

11 Scuola Normale Superiore, Pisa, Italy

cardiac malformations [2]. Recently, genome-wide association studies (GWAS) have linked common *TBX5* sequence variants to increased vulnerability to cardiac arrhythmias [3]. Indeed, Ma et al. [4] have found a strong relationship between *TBX5* mutations and atrial fibrillation (AF) in Caucasian and Chinese populations without cardiac malformations, supporting an independent role for TBX5 in modulating both cardiac development and electrophysiological properties.

In mice, alteration of *Tbx5* expression causes abnormal cardiac morphogenesis and changes in gene expression that correlate with *Tbx5* dosage [5]. The removal of TBX5 from the adult mouse caused primary spontaneously sustained AF in adult mice [6]. In zebrafish, homozygous *tbx5a* mutant embryos, or embryos injected with a morpholino against *tbx5a,* exhibit lethal defects in cardiac looping morphogenesis and the absence of pectoral fins [7], supporting an evolutionarily conserved role for Tbx5 function. Various animal models have revealed that TBX5 directly and indirectly controls an extremely complex network of genes, although the study of the molecular mechanisms associated with their functions is still in its infancy [8, 9]. Previously, we highlighted the importance of miRNAs in the Tbx5 regulatory circuit [10, 11, 12]. We showed that overexpression of miR-19a, which is downregulated in zebrafish Tbx5a morphants, was able to partially rescue cardiac and fin defects induced by Tbx5a depletion and to shift the global gene expression profile of *heartstring* embryos towards the wild-type condition. Since this analysis was performed at the whole embryo level, the effects of cardiac-specific miRNA replacement are still unknown. In this study, we detected cardiac upregulation of miRNA-182-5p in E11.5-E12 Tbx5 heterozygous mutant mice (a HOS model) compared to normal mice. Both transient and stable upregulation of miRNA-182-5p affected heart morphology and electrophysiological properties in zebrafish. Moreover, cardiac-specific downregulation of miRNA-182-5p limited the occurrence of defects in zebrafish HOS hearts, suggesting an evolutionarily conserved key role in regulating both heart development and its vulnerability to arrhythmias.

Methods

Mouse husbandry

Generation and genotyping of $Tbx5^{lox/+}$ mice have been previously described [5]. Mice with $Tbx5^{lox/+}$ alleles were maintained as inbred C57Bl/6. These mice were crossed to CAG-Cre transgenic mice [13] to generate $Tbx5^{del/+}$ mice on a C57Bl/6:129SvJ mixed genetic background. All animal experimental procedures conformed to the NIH guidelines and to the Institutional Animal Care and Use Committee at Weill Cornell Medical College.

NGS miRNA profiling

High-throughput RNA sequencing was performed on pools of E11.5-E12.0 WT, CRE, $Tbx5^{lox/+}$ and $Tbx5^{del/+}$ mouse dissected hearts (12 WT hearts, 9 CRE hearts, 13 $Tbx5^{lox/+}$ hearts, and 15 $Tbx5^{del/+}$ hearts, respectively). Three different total RNA extractions were carried out from WT, $Tbx5^{lox/+}$ and $Tbx5^{del/+}$ mouse dissected hearts and two for CRE hearts using the miRNeasy Mini Kit TRIzol (Invitrogen, Grand Island, NY) and purified using the PureLink RNA Mini kit (QIAGEN, Milan, Italy) according to manufacturer's instructions. RNA quantity and quality were assessed using the Agilent Technologies 2100 Bioanalyzer (Santa Clara, CA). NGS sequencing was performed on one pool per condition following the methodology described in [14]. The analysis of sequencing data was performed as described in [9]. Differential analysis was conducted using the Bioconductor's package DESeq [15] with the assumption that, in the absence of replicates, there is no true differential expression for most genes, and that a valid mean–variance relationship can be estimated from treating the two samples ($Tbx5^{lox/+}$ or $Tbx5^{del/+}$ mouse hearts versus WT and CRE mouse hearts, respectively) as if they were replicates as suggested in [15]. To this end, we used the estimate Dispersions function with method = "blind" and sharing Mode = "fit-only" parameters setting. The validation of modulated miRNAs was performed by Q-PCR on all three different pools for each genetic background.

Maintenance of Zebrafish lines

The zebrafish facility has held the authorization n 297/2012-A since 12/21/2012. All the experimental protocols were approved by the Italian Ministry of Health (protocol ADRP n.0000223 and protocol ADPR n.0000222). All animal procedures conform to the guidelines from Directive 2010/63/EU of the European Parliament regarding the protection of animals used for scientific purposes. *Wild-type AB, Tg(myl7:EGFP), Tg(myl7: nuDsRED), Tg(flk1:EGFP), Tg(myl7:gCaMP)* and $Tbx5^{as296}$ transgenic zebrafish lines were used in this study.

Euthanasia

Pregnant mice were killed by CO_2 delivery followed by cervical dislocation before isolation of embryonic day (E) 11.5–12.0 embryos. The embryos were killed by cervical dislocation. To euthanize embryonic fish, bleach solution (sodium hypochlorite 6.15%) was added to the culture system water at 1 part bleach to 5 parts water, and the larvae

were left in this solution at least 5 min prior to disposal to ensure death.

Physiological analysis

Once anesthetized, transgenic *Tg(myl7:EGFP)* zebrafish embryos (2/3/6dpf) were transferred to a 35-mm Petri dish and mounted in 1% low-melting agarose. Fluorescence analysis was performed with an Eclipse E600FN Nikon microscope (excitation 480 nm, emission 510 nm, objective 20x). Images were recorded by a CCTV camera Panasonic WV-BP514, AD converted by a frame grabber interface board (Image Lightning 2000), analyzed by the software Imaging Workbench 2.1 (Axon, USA). Videos were acquired at 25 frames per second. Frames were analyzed by LabVIEW software developed for this microscope. The heart rate was measured over a time course by tracking signal changes in selected Regions of Interest (ROIs). Alternatively, a photomultiplier (CAIRN, Research, UK) was used to measure the changes in intensity of fluorescence emission in a single selected ROI.

For calcium imaging we incubated transgenic *Tg(myl7:gCaMP)* embryos in 20 mM of 2,3-butanedione monoxide for 20 min before the analysis to stop cardiac contraction [16, 17].

For time-lapse experiments, frames were acquired using a Zeiss spinning disk confocal microscope system with CSU-X1 (Yokogawa) and ORCA-flash 4.0 sCMOS cameras (Hamamatsu). Zebrafish embryos were injected with the morpholino against the troponin T (see Table S1 for sequence) to stop contraction. The fluorescence emission intensity was measured based on a profile positioned along the atrio-ventricular axis, and the time course of the calcium wave was measured.

Electrocardiogram recording

ECG recordings were performed on anesthetized (0.04% tricaine) zebrafish embryos (2/3/6 dpf) immobilized in a groove of agarose. The tip of a glass micropipette (diameter 2 µm) was positioned on the pericardial surface between the atrium and ventricle. Two silver chloride electrodes were inserted in the pipette and in the bath and connected to a differential amplifier (WPI DAM-6A, filtering 0.1 Hz–3 kHz). Data were acquired by a PCI-6251 card (National Instruments) and processed on line by software developed in LabVIEW.

Statistics

Statistical analysis was performed using analysis of variance or Student's *t* test. The χ^2 test was used to asses rescue experiments in the mutant line and for in situ hybridization classified with nominal data. For rescue experiments, the theoretical probability of all phenotypes in relation to the respective genotype was previously quantified in the *Tg(GAL4/miR-182)* transgenic line for a population derived from a cross between parents heterozygous for two different genes, assuming a coherent condition with Hardy–Weinberg equilibrium. The Student's *t* test was performed by multiplying the values of each inferred class with the theoretical probability found in the genetic analysis of population. We adopted *for $p < 0.05$; **for $p < 0.01$; ***for $p < 0.001$; ****for $p < 000.1$.

Results

miR-182-5p is upregulated in hearts of HOS mouse model

To identify miRNAs involved in *Tbx5* cardiac regulatory circuits, Next Generation Sequencing (NGS) miRNA profiling was performed on RNA isolated from whole WT, CRE/+, $Tbx5^{lox/+}$ and $Tbx5^{del/+}$ E11.5–E12.0 mouse hearts. WT and CRE/+ mouse hearts shared comparable *Tbx5* expression levels (Fig. 1a) and were used as control groups for $Tbx5^{lox/+}$ and $Tbx5^{del/+}$, respectively. We analyzed hearts from these mice to identify miRNAs that are differentially modulated in response to varying gene dosages of *Tbx5* since cardiac expression is finely modulated by the *Tbx5* gene in a dose-sensitive manner [8]. In $Tbx5^{lox/+}$ mouse hearts harboring a hypomorphic allele of *Tbx5*, we identified five miRNAs significantly upregulated in comparison to WT hearts. $Tbx5^{del/+}$hearts, which are haploinsufficient for *Tbx5*, showed 10 upregulated and 1 downregulated miRNAs compared to CRE/+ mouse hearts (Figs. 1b and S2A). MiR-182-5p, miR-375-3p, miR-10a-5p, and miR-183-5p were significantly upregulated in both $Tbx5^{lox/+}$ and $Tbx5^{del/+}$mouse hearts. These data were validated by Quantitative Real-Time PCR (Q-RT PCR) (Fig. S2B).

Because of mir-182-5p's robust cardiac expression and evolutionary conservation (Fig. S2C), we decided to further investigate its role in the Tbx5 regulatory circuit. MiR-182 was highly up-regulated by over fourfold in both $Tbx5^{del/+}$ and $Tbx5^{lox/+}$ hearts, suggesting that this miRNA is acutely sensitive to minor *Tbx5* perturbations [8]. MiR-182 is a member of the miR-183–96–182 cluster (miR-183 cluster). The other paralogs of this cluster (miR-183 and miR-96) show lower expression levels compared to miR-182 (www.mirbase.org) and were also upregulated in *Tbx5*-deficient hearts (Fig. 1b). This finding suggested that TBX5 negatively controls the expression of the entire miR-183 cluster. The role of TBX5 as a transcriptional repressor was recently substantiated by the TBX5 interactome analysis [18]. Because Kruppel-like factor 4 (KLF4) is directly repressed

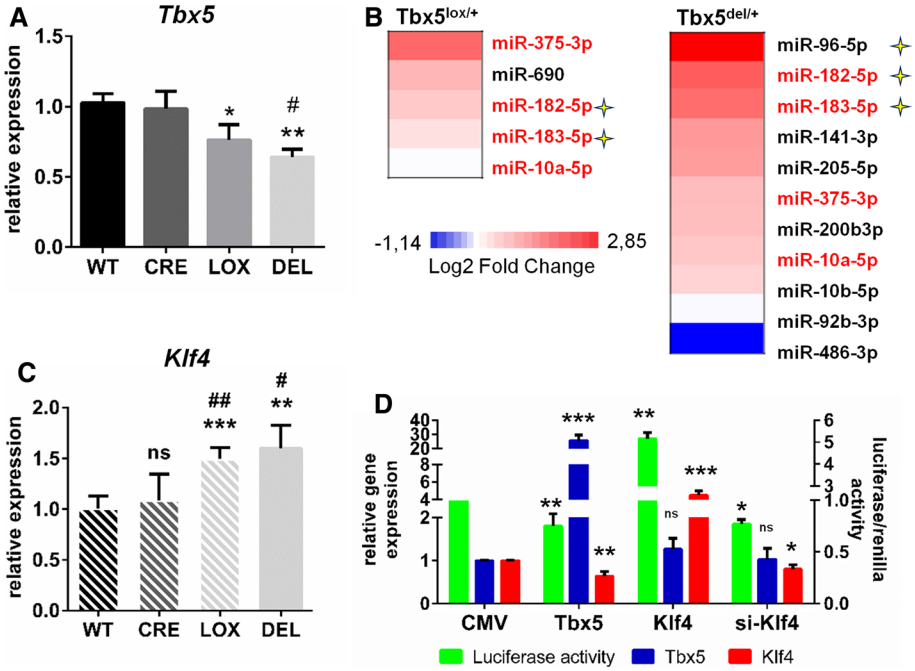

Fig. 1 Tbx5 downregulation alters miRNA expression in embryonic mouse hearts. **a**, **c** Q-RT PCR analysis of Tbx5-exon 3 and Klf4 expression in E11.5–12.0 mouse hearts. Three heart pools for each genotype were analyzed. *t* test $*p<0.5$, $**p<0.01$ vs WT; $\#p<0.5$ vs CRE. (B) Heat map of differentially expressed miRNAs in E11.5-E12 $Tbx5^{lox/+}$ vs WT and $Tbx5^{del/+}$vs CRE/+ mouse isolated hearts. MiRNAs were differentially modulated by varying degrees among both genotypes (shades of red). Asterisks indicate miRNAs of the miR-183 cluster. **d** Transactivation assay of the miR-183 cluster promoter in HL-1 cells co-transfected with CMV empty vector or CMV vectors expressing Tbx5, Klf4 or a siRNA for Klf4. Green Luciferase activity, and Q-RT PCR quantification of Tbx5 (blue) and Klf4 (red) in transfected cells is presented. The values reported represent the mean of three independent transfection experiments. Statistics: *t* test $*p<0.05$; $**p<0.01$; $***p<0.001$

by TBX5 and regulates the miR-183 cluster in both physiologic and pathologic conditions [19], we hypothesized that TBX5 deficiency might upregulate the miR-183 cluster by relieving repression of KLF4. We confirmed that KLF4 is upregulated in the myocardium of TBX5-depleted mice (Fig. 1c). In accordance with our hypothesis, we observed that KLF4 transcriptionally activated a luciferase reporter vector containing a 3.2-kb region derived from the 3′-flanking region of the predicted start site of the miRNA-183 cluster. Conversely, KLF4 siRNA caused opposite effects on the reporter construct containing the miRNA-183 cluster promoter. Consistent with our hypothesis, *Tbx5* overexpression in HL1 cells repressed the transcription of the above mentioned luciferase reporter and *Klf4* expression (Fig. 1d). Together, our data suggest that TBX5 contributes to miR-183 cluster regulation plausibly through KLF4 modulation.

A few data concerning the miR-182 role in cardiac context further stimulate our interest in this microRNA: by reprocessing published NGS analysis, we identified significant miR-182 upregulation in hearts of ischemic or non-ischemic failing patients compared to healthy subjects [20]. Moreover, microarray profiling indicates that high levels of circulating miR-182 might have a prognostic value in human heart failure [21] and, more recently, miR-182 was shown to modulate the myocardial hypertrophic response in a mouse model of angiogenesis-induced hypertrophy [22]. The only data concerning a possible role of miR-182 in cardiac development concern the downregulation of miR-182 during the maturation process of human embryonic stem cell-derived cardiomyocytes [23]. This prompted us to broaden our initial investigation of miR-182 in the murine heart to determine its evolutionarily conserved cardiac role in other species. We chose the zebrafish model because it offers many advantages for investigating vertebrate development and modeling human disease [24].

miR-182 overexpression impacts zebrafish heart development

To examine the role of miR-182 in zebrafish heart development, we performed gain- and loss-of-function experiments. We microinjected increasing amounts of miR-182 or miR-CT mimics into *Tg(myl7:EGFP)* embryos [25]. At 72 hpf, miR-182 overexpressing (miR-182-OE) embryos showed severe cardiac edema and a dose-dependent increase in heart defects (Figs. 2a, and S3A, B). However, these miR-182-OE embryos exhibited normal vascular patterning and pectoral fins (Fig. S3D, E, F). We documented three main

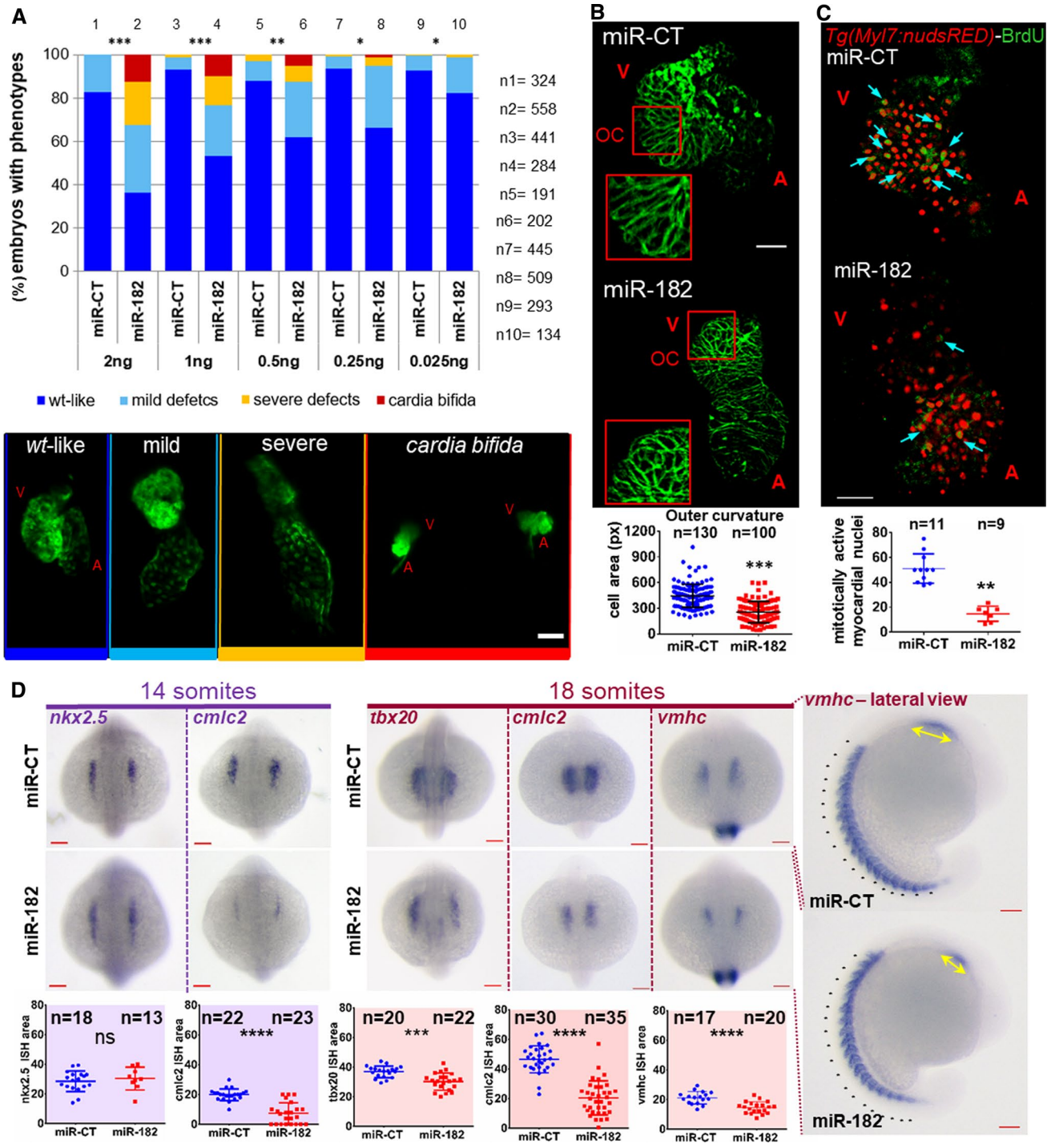

Fig. 2 MiR-182 overexpression affects cardiac development. **a** *Tg(myl7:EGFP)* embryos were injected with increasing amounts of miR-182 or miR-CT mimics. Confocal images of representative 72 hpf embryos show varying degrees of severity of heart defects. Top, quantification of different phenotypes. **b** Confocal images showing cell morphology after phalloidin immunostaining and quantification of cell areas of 11 embryos injected with miR-CT (130 cells counted) or 11 embryos injected with miR-182 ($n=110$ cells counted). Scale bar = 40 µm. **c** BrdU assay in dissected *Tg(myl7:nuDsRED)* hearts at 48hpf, after mimic injection. Top, confocal images after immunostaining with anti-BrdU antibody (green). Light blue arrows point to examples of cardiomyocytes that incorporated the BrdU in the red nucleus. Scale bars = 50 µm. Bottom, double labeled cell quantification. **d** Whole mount ISH analysis of early markers of cardiac development in miR-CT and miR-182 injected embryos. Scale bars = 100 µm. Bottom, relative ISH area quantification. Statistics: Fisher's test $p<0.0001$; *t* test $^{*}p<0.05$; $^{**}p<0.01$; $^{***}p<0.001$

classifications of heart defects among the miR-182-OE embryos. MiR-182-OE embryos classified as "mild" principally demonstrated failed cardiac looping but normal cardiac ballooning in the atrium and ventricle. Embryos scored as "severe" showed looping defects together with abnormal cardiac ballooning (in one or both cardiac chambers); these embryos ultimately developed a highly stretched heart. This heartstring-like phenotype was morphologically similar to the one observed in Tbx5 depleted zebrafish embryos (Fig. S3C [7, 11],). *Cardia bifida* was observed in a few embryos at higher miRNA doses. Additional examples of observed cardiac phenotypes are shown in Fig. S4. Next, we examined myocardial cell morphology using phalloidin immunostaining to label the actin cytoskeleton. Confocal microscopy of wild-type (wt) embryos at 48 hpf revealed that wild-type ventricular cells along the outer curvature (OC) appeared elongated [26]. MiR-182-OE embryos OC ventricular cells failed to elongate and showed a significantly smaller cell size than wt embryos at 48hpf (Fig. 2b). This analysis suggests an alteration of cardiomyocyte maturation caused by miR-182 overexpression (Fig. 2b). In contrast to phenotypes associated with miR-182 gain-of-function, miR-182 loss-of-function phenotypes obtained by miR-182 morpholino (MO-182) injection did not produce any gross cardiac morphological defects (Fig. S5A, B) nor did it affect fin development (Fig. S5C). The efficacy of MO-182 was demonstrated by its ability to counteract cardiac defects induced by miR-182 overexpression (Fig. S5D).

To investigate whether miR-182 overexpression might affect the cardiomyocyte differentiation process, we analyzed the expression of cardiac markers at early and late developmental stages by in situ hybridization (ISH). Cardiac lineage in progenitor cells was assessed by the expression of *nkx2.5*, a marker of precardiac mesoderm [27]. The bilateral heart field of *nkx2.5* expression at the 14 somite stage (14ss), both in miR-182- or miR-CT-injected embryos, did not differ distinctly. Conversely, expression of *cardiac myosin light chain 2* (*cmlc2/myl7)* was strongly reduced by miR-182 overexpression, as was *ventricular myosin heavy chain (vmhc)* and *tbx20* expression at the 18ss (Fig. 2d). These expression data, along with the myocardial morphology findings, suggest that miR-182 overexpression does not affect the specification of cardiac precursors. Rather, miR-182 regulates myocardial differentiation, which is one of the key cardiac developmental processes that TBX5 governs [28, 29]. Next, we analyzed the levels of several cardiac markers known to be altered in *tbx5*-deficient embryos [7, 30] at 48 hpf stage. We found substantial overlap in the patterns of expression between *tbx5*-deficient embryos and miR-182-OE embryos for the majority of the tested genes (Fig. S6A, B). First, the *tbx18* and *wt1* proepicardial markers showed reduced expression relative to wt hearts (Fig. S6). Next, myocardial *versican a* and endocardial *notch 1* expression significantly expanded into the cardiac chambers of miR-182-OE embryos. In wt embryos, expression of *versican* and *notch 1* is restricted to the atrioventricular junction at this stage. (Fig. S6, [10, 30]). In addition, the normal restriction of *bmp4* expression to the atrioventricular boundary after 37 hpf does not occur in miR-182-OE embryos, as likewise observed in Tbx5a mutants or morphants. The myocardial marker *nppa*, whose expression is reduced in *tbx5*-deficient embryos, did not substantially change its expression pattern, although the expression level appeared higher in the atrium, whereas wt hearts typically exhibit dominant expression in the ventricle (Fig. S6). Overall, our analyses show that overexpression of miR-182 alone is sufficient to induce cardiac expression patterns which resemble the *hst* expression pattern.

To investigate whether cardiac defects caused by miR-182 overexpression reflected an altered cardiomyocyte proliferation rate, we used bromodeoxyuridine (BrdU) incorporation to assay for actively proliferating cells [31]. 1-cell stage embryos of the *Tg(Myl7:nuDsRED)* transgenic line were microinjected with 0.5 ng of miR-182 or miR-CT mimics and allowed to incorporate BrdU from 36 to 48 hpf. Red fluorescent protein in the nucleus of myocardial cells was used to count the number of cells present. Results presented in Fig. 2c show that miR-182 overexpression significantly reduced myocardial cell proliferation.

The *cardia bifida* phenotype that we observed in miR-182-OE embryos (Fig. 2a) suggests a possible defect in myocardial cell migration during the formation of cardiac ring. To examine dynamic cell movements during heart tube assembly, we performed *nkx2.5* ISH at time-points before cardiomyocytes approach the embryonic midline (see Sect. 3.8 in supplementary methods and Fig. S1). We found reduced migration of myocardial precursors in miR-182-OE embryos during the early phase of the migration process (15–18ss) (Fig. S7). On the whole, these results indicate that zebrafish miR-182 is deeply involved in crucial processes for cardiac morphogenesis.

Similarly, Q-RT PCR assays using mouse cell lines transfected with miR-CT or mir-182 showed that several markers of cardiac differentiation are differentially expressed in miR-182 transfected cells (Fig. S8A). Moreover, a wound closure assay indicates a reduced ability of miR-182 injected cells to migrate, relative to miR-CT cells (Fig. S8B). These findings are consistent with the premise that some of miR-182 functions are conserved in mammalian cells.

miR-182 depletion partially rescues cardiac defects in both Tbx5a mutant and morphant embryos

In accord with miRNA profiling in mouse HOS model, zebrafish miR-182 and *klf4* appears significantly increased in hearts isolated from 48 hpf MO-Tbx5a embryos compared

to those of control morphants as detected by Q-RT PCR (Fig. 3a). ISH analysis supported the upregulation of *klf4,* in particular showing an alteration of *klf4* pattern expression in hearts of MO-Tbx5a embryos (Fig. 3c). The miR-182 ISH data confirm the cardiac expression of this miRNA, although miR-182 modulation in the tbx5a morphants was less evident and the expression pattern does not seem altered (Fig. 3b). However, it is well known that ISH is not quantitative technology, and ISH can be challenging for miRNA analysis, given their short length [32]. Interestingly, several putative *klf4* binding sites were identified in the miRNA-183 cluster promoter by Jaspar analysis (Fig. S9A–C). Consistent with this observation, cardiac levels of miR-182 increased after *klf4* overexpression (Fig. S9D) and cardiac but not fin defects were observed (Fig. S9E). Overall these data suggest a positive regulation by Klf4 on miR-182 expression in zebrafish embryos. Starting from these observations, we reasoned that if Tbx5 negatively regulates miR-182, some of the cardiac defects caused by Tbx5 depletion in zebrafish might be ameliorated by restoring the negative control upon this miRNA. To verify this hypothesis, we performed rescue experiments, exploiting *tbx5a*^{s296} mutant line in which homozygous embryos develop the *heartstring* phenotype and lack pectoral fins, while heterozygous embryos are

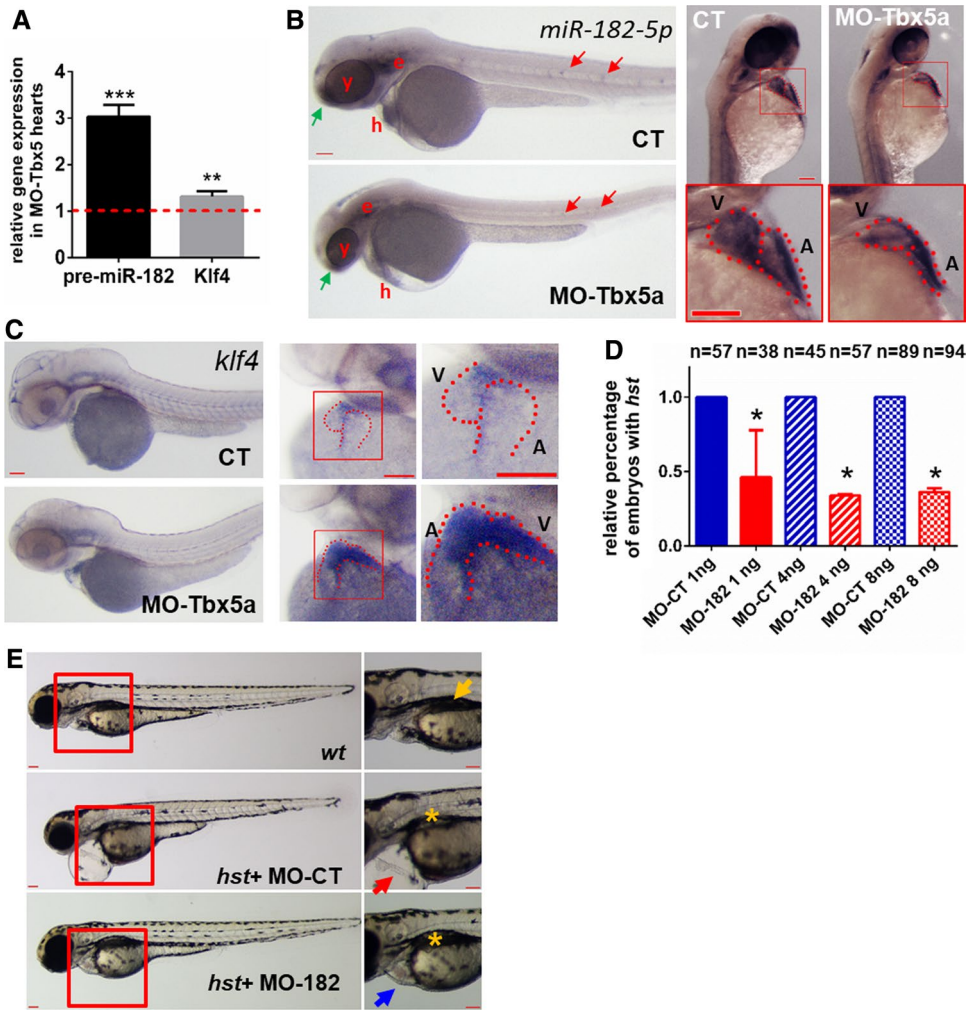

Fig. 3 miR-182 depletion is able to partially rescue cardiac defects in Tbx5a mutant embryos. **a** Q-RT PCR quantification of pre-miR-182 and klf4 in hearts isolated from MO-Tbx5a 48hpf embryos compared to MO-CT hearts. About 150 isolated hearts for each treatment were analyzed. Student's *t* test $^{**}p<0.01$; $^{***}p<0.001$. **b** ISH of miR-182 in control and MO-Tbx5a embryos. Letters and arrows point to body regions where miR-182 is expressed: e = ear, y = eye, h = heart, red arrows point to ganglia, green arrow points to a frontal region of nervous system. On the right heart magnification. Scale bars = 100 µm. **c** ISH of *klf4* in control and MO-Tbx5a embryos. Left = lateral view, right = frontal view of heart magnification. Scale bars = 100 µm. **d** Analysis of 72 hpf *Tbx5a*^{s296} mutant embryos injected with MO-CT or MO-182 at the reported doses. Only "no fin" embryos were included in the analysis. χ^2 test $^{*}p<0.05$. **e** Images representative of *Tbx5a*^{s296} mutant embryos after injection of 4 ng of MO-CT or MO-182. On the right, the higher magnifications highlight fin presence (yellow arrow), fin absence (yellow asterisks), as well as the *heartstring* cardiac phenotype (red arrow) which has been rescued in MO-182 morphant hearts (blue arrow). Red scale bar = 100 µm

phenotypically normal. Since homozygous *tbx5a*^{s296} fish do not reach sexual maturity, we performed all the experiments by crossing heterozygous *tbx5a*^{s296} fish. Because heterozygous *tbx5a*^{s296} embryos always generate normal pectoral fins and because MO-182 injection does not affect fin development in wt (Fig. S5C), we were able to use the absence of pectoral fins as a clear indicator of that embryos were homozygous mutant for *tbx5*. Rescue analysis was restricted only to embryos lacking pectoral fins. The percentage of embryos with *heartstring* phenotypes was significantly reduced, whereas the percentage with wt-like or mild phenotypes increased in MO-182 injected, relative to MO-CT injected *tbx5a* mutant embryos (Figs. 3d, e and S10A). These results were confirmed by rescue experiments performed in *tbx5* morphants and by the ISH analysis of some cardiac markers (Fig. S10B–D). Altogether, our data demonstrate that miR-182 is part of the *tbx5* regulatory circuit.

Identification of miR-182 putative targets

To search for miR-182 targets in cardiac development, we performed an in silico analysis in mouse and zebrafish using predictive algorithms and combined the results as summarized in Fig. S11A. This study produced a list of 4351 putative miR-182 targets, 548 of which are shared between mouse and zebrafish. The complete list of the putative miR-182 targets were used as queries to search the KEGG (Kyoto Encyclopedia of Genes and Genomes) database. We found at least one associated KEGG pathway for 1730 putative targets (Table S1). Apart from very general categories such as metabolic pathways or pathways in cancer, the enrichment analysis (reported in Fig. S11B) identified several pathways known to play important roles also in cardiac development and function, including the Wnt signaling pathway [33, 34], the PI3K-Akt and mTOR signaling pathways [35, 36], regulation of actin cytoskeleton [37], calcium signaling [38] and others. However, since we mostly observed cardiac defects caused by miR-182 overexpression during the zebrafish developmental stage under investigation, we focused on four highly represented KEGG pathways related to cardiac pathologies: hypertrophic cardiomyopathy, dilated cardiomyopathy, arrhythmogenic right centricular cardiomyopathy, and adrenergic signaling in cardiomyocytes. Out of 1730 putative targets, 76 genes matched at least one cardiac-associated KEGG pathway and 12 genes matched all four KEGG pathways (Fig. S12B). Remarkably, 10 out of the 12 genes are calcium channel subunits or genes involved in calcium homeostasis. It is noteworthy that calcium signaling is also one of the enriched KEGG pathways highlighted in Fig. S11B. To support this analysis, the expression of a subgroup of putative targets that showed the highest target site predictive values (Fig. S12B) and that were identified as targets in both mouse and zebrafish, was quantified in hearts isolated from 48 hpf embryos by digital droplet PCR. A significant decrease in mRNA levels for *cacnb2.2*, *cacnb4b* and *cacna2d1* was observed in miR-182-OE hearts compared to control hearts (Fig. 4a). ISH analysis supported the *cacnb4b* and *cacna2d1* downregulation in miR-182 OE hearts (Fig. S14). By luciferase reporter assay, we showed that *cacna2d1* is a direct target of miR-182 (Fig. S13A).

miR-182 overexpression affects heart physiology

Since alteration in L-type calcium channels (LTCC) can impact cardiac development [31, 39], we hypothesized that dysregulation of these genes might be at the root of the cardiac morphology defects observed in miR-182-OE embryos. Moreover, alterations of LTCC subunits may increase cardiac vulnerability to arrhythmias, as already observed in diabetic mice [40]. To test this hypothesis, we assessed cardiac performance in *Tg(myl7:EGFP)* embryos injected with 0.5 ng of miR-182 or miR-CT. MiR-182-OE embryos showed a decrease in average heart rate at 72 hpf (Fig. S13B), although embryos with tachycardia and heart block were also identified. Overall, about 50% of embryos showed altered heart rate (Fig. 4b).

To investigate the effects of miR-182 in heart physiology in greater detail, we recorded a time course of atrial and ventricular contractions using fluorescence microscopy. We analyzed hearts at 72 hpf, selecting only the wt-like/mild hearts among the miR-182-OE embryos to limit the secondary impacts of cardiac defects on organ function. miR-CT injected hearts produced a regular heart rate (Fig. 4C1). Among the miR-182-OE embryos, we observed several cases of arrhythmias in almost all replicates, although affected embryos displayed high variability regarding the duration and the severity of the arrhythmic phenomena. In some cases, we observed a burst of mechanical activity followed by sinus pauses lasting for several seconds, combined with beats occurring at an irregular rate (Fig. 4C2). We repeated this analysis at 6dpf and again observed intermittent rhythms in a high percentage of miR-182-OE embryos (Fig. S13C). To investigate whether the heart arrhythmias we observed might be related to calcium handling alterations, we conducted a similar analysis in the *Tg(myl7:gCaMP)* line [16] on embryos treated with 2,3-butanedione monoxide to block myocardial contraction [16]. As predicted, we observed alterations in the rate of cardiac calcium waves in miR-182-OE embryos (Fig. 4C4), confirming that calcium handling is affected in miR-182-OE hearts. We repeated the analysis blocking contraction by microinjecting a morpholino against the Troponin T (MO-Tnnt2a) [41]. Using confocal microscopy, we acquired stacks of time-lapse imaging in 48 hpf embryos previously microinjected with 0.5 ng of miRNA mimic, together with 2 ng of MO-Tnnt2a to prevent contraction. We observed

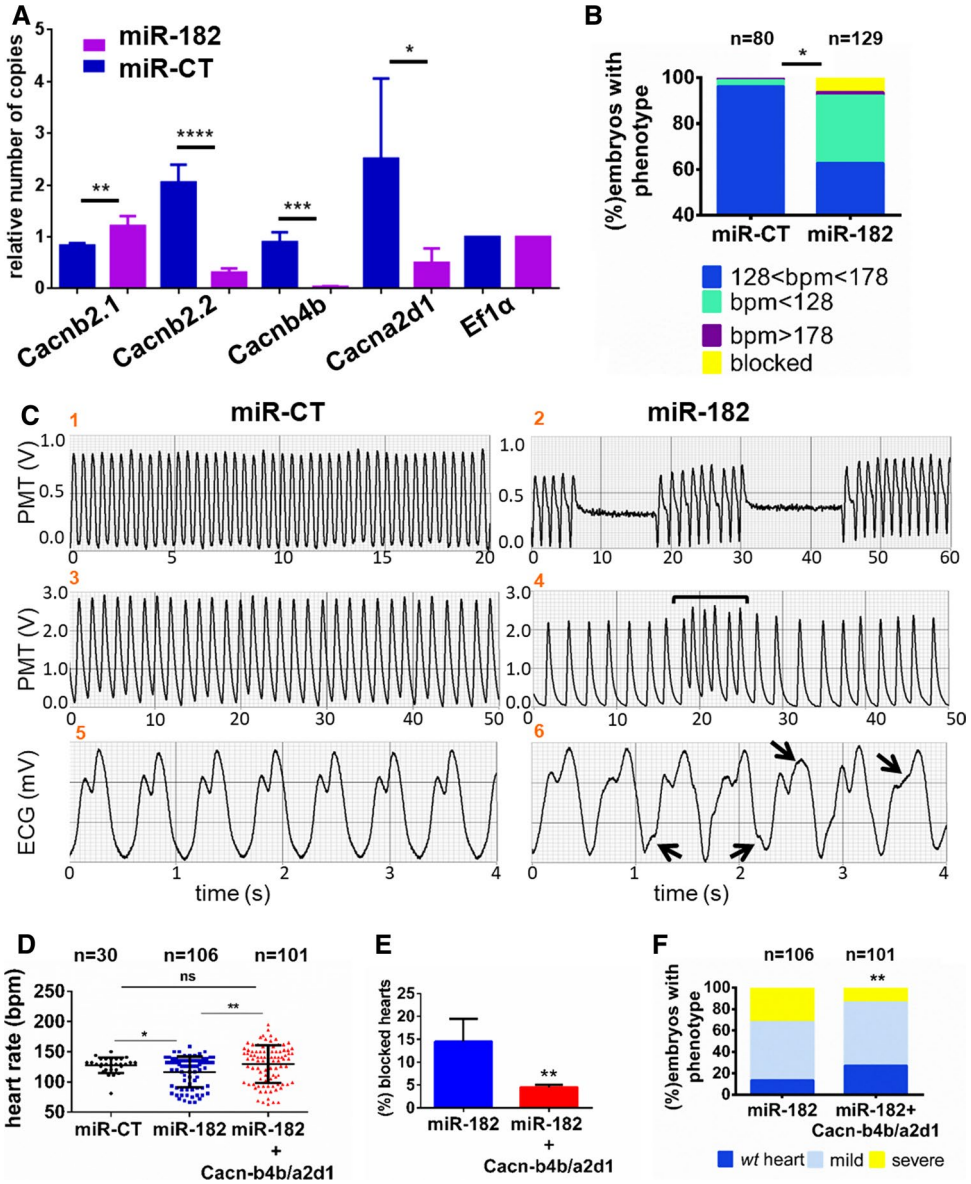

Fig. 4 MiR-182 overexpression affects heart physiology. **a** DdPCR analysis in RNA extracted from hearts dissected from 48 hpf embryos microinjected with 0.5 ng of miR-182, or miR-CT. Data show the number of copies in 1 µg of extract and are relative to ef1α copy number. About 30 isolated hearts for each treatment were analyzed. **b** Analysis of heart rate (beats per min, bpm) in 72hpf embryos microinjected with 0.5 ng of miR-182, or miR-CT. A quantification of the different classes of heart rate frequency is presented. **c** C1,C2 show heart rate recorded by a photomultiplier in a miR-CT or in a miR-182 injected *Tg(myl7:EGFP)*embryo, respectively. The activity is regular in 1 whereas is bursting in 2. Note irregular periods inside bursts. Systole is indicated as upward deflection. C3,C4 show intracellular calcium oscillations recorded by a photomultiplier during the heart cycle in a miR-CT and a miR-182 injected *Tg(myl7:gCaMP)* embryo, respectively. In C4 an episode of arrhythmia is marked with a bracket. C5,C6 represent ECG recording from 72hpf zebrafish microinjected with miR-CT or miR-182, respectively. The arrows indicate abnormal shapes of ECG waves. **d–f** Analysis of heart rate (**d**), relative percentage of blocked heart number (**e**) and heart morphology (**f**) in 5dpf embryos microinjected with 0.5 ng of miR-182 in the presence or not of 5 pg of in vitro transcribed *cacnad2a1* together with 5 pg of *cacnb4b*. Statistics: Student's *t* test $*p<0.05$; $**p<0.01$; $***p<0.001$

that the falling phase of the calcium wave in miR-182-OE embryos (Fig. S13D4–6) spanned a longer period of time than in controls (Fig. S13D1–3). In support of this observation, injection of a mixture of *cacnb4b* and *cacna2d1* mRNAs ameliorated heart morphology defects and regularized heart rhythm in miR-182-OE embryos. Importantly, the onset of heart block was significantly reduced in treated animals (Fig. 4d–f). Since the alterations of the mechanical activity in miR-182-OE embryos might be due to defective sarcomeric molecular machinery and/or to malfunction of myocyte electrogenesis, ECG was used to assess the heart electrophysiology. ECG recordings from larval zebrafish

(72 hpf) microinjected with miR-182 showed an irregular shape of ECG waves (Fig. 4C6). Overall, these data demonstrate that miR-182 overexpression affects not only heart development but also cardiac function.

Cardiac-specific overexpression of miR-182 alters cardiac phenotype

To further investigate the consequences of cardiac miR-182 dysregulation, we generated two transgenic lines that stably overexpress or downregulate miR-182 in cardiomyocytes (Fig. S15A). The expression of miR-182 or its specific sponge (8 repeats of miR-182 binding sites) in both *Tg(GAL4/miR-182*) and *Tg(GAL4/sponge-miR-182)* lines, was activated by GAL4 under the control of the strong *myl7* cardiac promoter. MiR-182 modulation in the transgenic hearts was verified by Q-RT PCR quantification (Fig. S15B) and by functional tests (Fig. S15C).

We first analyzed the cardiac morphology of the transgenic lines we generated and did not initially detect cardiac defects in 72hpf *Tg(GAL4/miR-182)* and *Tg(GAL4/sponge-miR-182)* embryos. After back-crossing *Tg(GAL4/miR-182)* adults, however, mild cardiac defects were detectable in 30% of 72hpf F1 embryos with green eyes and heart, i.e., those that overexpressed miR-182 (Fig. 5a). In addition, the *Tg(GAL4/miR-182)* line showed a significant reduction in viability (Fig. S15D). By comparison, the *Tg(GAL4/sponge-miR-182)* fish appeared normal after back-crosses; embryos showed normal heart development, but a similar reduction in viability. Embryos of *Tg(myl7:GAL4)* and *Tg(UAS:sponge-miR-182)* control lines showed normal viability (Fig. S15D). Next, we tested the physiological activity of the transgenic hearts. At 72 hpf the hearts of heterozygous *Tg(GAL4/miR-182)* embryos beat regularly. Likewise, in the F2 population, arrhythmic events were detectable in less than 1% of embryos, suggesting that only double homozygous embryos demonstrate higher susceptibility to arrhythmias. However, 6 dpf *Tg(GAL4/miR-182)* embryos revealed alterations of rhythm: these ranged from desultory (Fig. 5B2) to widespread (Fig. 5B3). Such variant rhythms were absent in *Tg(myl7:GAL4)* control embryos (Fig. 5B1). 60% of heterozygous fish and 80% of fish derived from an F2 backcross presented arrhythmias with high variability in the severity of the phenotype. ECG recordings from 6 dpf *Tg(GAL4/miR-182)* embryos revealed in several cases exhibiting a 2:1 activity pattern, alternating cycles with normal and attenuated P and R waveforms (Fig. 5B5). These data confirm the malfunction of myocyte electrogenesis.

According to the hypothesis that alteration in calcium handling might be primarily responsible for the *Tg(GAL4/miR-182)* cardiac defects, injection of a mixture of *cacnb4b* (5 pg) and *cacna2d1* (5 pg) mRNAs was able to reduce the cardiac defects in *Tg(GAL4/miR-182)* embryos by more than 70%, which aligns with our observations on transient miR-182-OE embryos. In contrast, this treatment worsened the *Tg(myl7:GAL4)* embryo phenotype (Fig. 5c).

Cardiac expression of miR-182-sponge significantly reduce the cardiac defects caused by tbx5a depletion

To further test whether cardiac-restricted expression of sponge-miR-182 was able to rescue cardiac defects caused by *tbx5a* depletion, we injected MO-Tbx5a in *Tg(GAL4/sponge-miR-182)* embryos and in *Tg(myl7:GAL4)* embryos as control. Although *Tg(myl7:GAL4)* embryos exhibited sensitivity to *tbx5a* depletion similar to wt embryos, MO-Tbx5 injected into *Tg(GAL4/sponge-miR-182)* embryos doubled the number of embryos with normal hearts and decreased the onset of mild or severe cardiac defects compared to wt AB embryos (Fig. 5d). These results accord with our previous data showing that MO-182 injection can rescue *tbx5* mutant and morphant cardiac defects (Fig. 3 and S10). Taken together, our data demonstrate that the cardiac modulation of miR-182 is able to impact the HOS phenotype, strengthening the hypothesis that miR-182 plays an active role in the *tbx5a* regulatory circuit.

Discussion

In this study, we show that miR-182 is upregulated in embryonic cardiac tissue of both mouse and zebrafish HOS models. Our functional analysis revealed that overexpression of miR-182 in zebrafish affects both cardiac morphology and electrical activity, whereas cardiac-specific downregulation of miR-182 in zebrafish HOS hearts attenuates cardiac defects. Our findings reveal a hitherto unsuspected evolutionarily conserved role of miRNA-182 in preserving the structural and electrical integrity of the myocardium.

To analyze the impact of increased miR-182 expression in zebrafish cardiac development, miR-182 was overexpressed in zebrafish embryos. The results highlighted a significant overlap of miRNA-induced cardiac alterations with defects caused by Tbx5 depletion. MiR-182-OE embryos show a dose-dependent onset of the heartstring phenotype and alterations in myocardial cell morphology. In assays of late cardiac genes known to be affected by Tbx5, 5 out of 6 genes showed the same altered pattern as observed in miR-182 OE embryos. In line with *hst* mutant phenotypes, miR-182-OE embryos developed correct specification of cardiac progenitors but presented reduction in differentiation markers, in particular *myl7,* which is not reported to be affected in *hst* mutants. However, it is interesting to note that *myl 7* is one of the genes identified as downregulated in mouse HOS hearts [8]. Moreover miR-182 overexpression

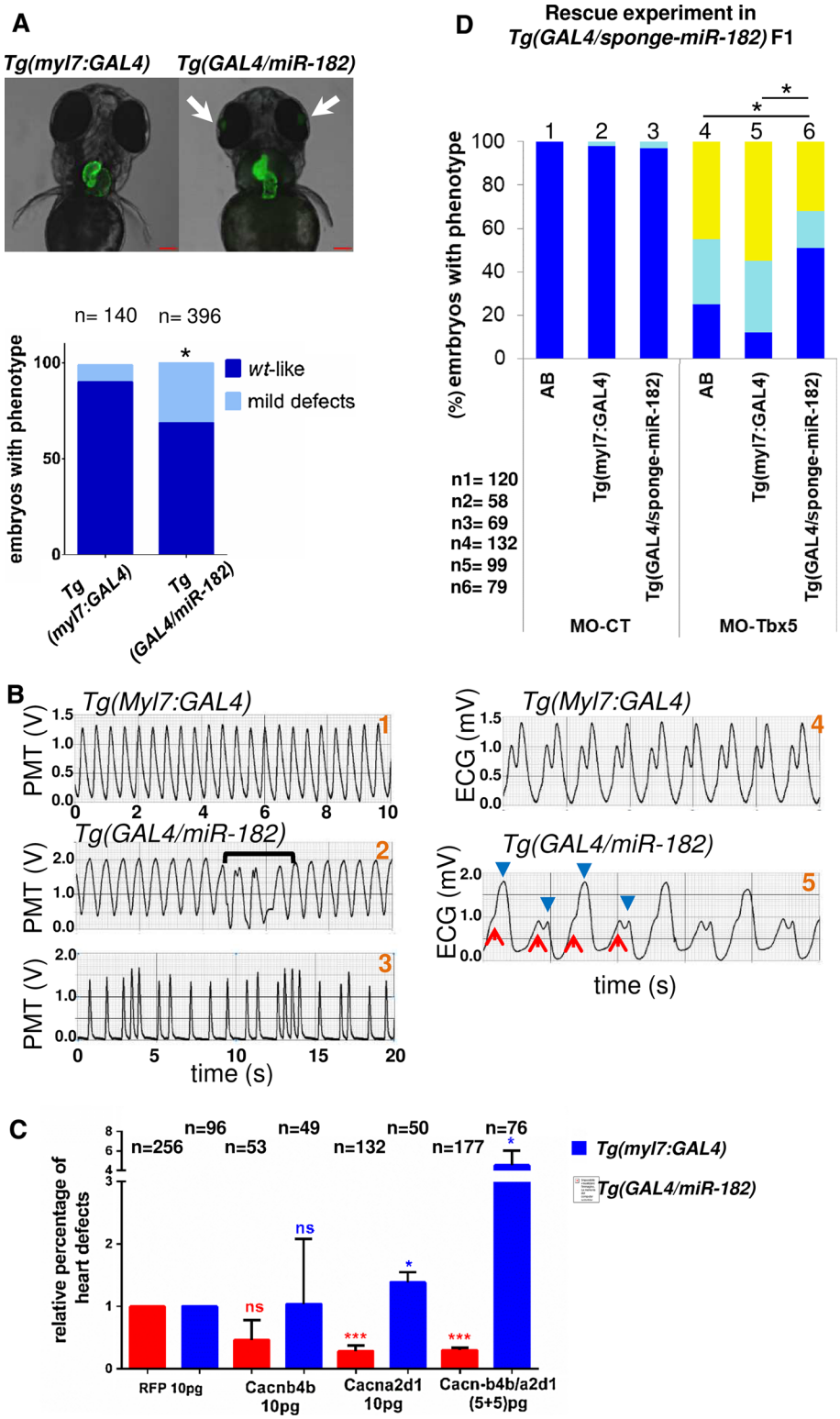

Fig. 5 Stable cardiac-specific overexpression of miR-182 affects heart morphology and activity. **a** Top, 72hpf F2 transgenic embryos. White arrows point to GFP expression in the lens of the eyes. Scale bar = 100 µm. Bottom, quantification of embryos showing heart defects. **b** Left, mechanical activity recorded from a 6 dpf *Tg(myl7:GAL4)* embryo, as control (1), and from *Tg(GAL4/miR-182)* embryos (2, 3). Systole is indicated as upward deflection. Right, ECG recorded from a control embryo (4) and from a transgenic embryo (5). In 5, the non-equal P and R peaks are indicated by upward and downward arrows, respectively. **c** Relative reduction in heart defects in F2 *Tg(GAL4/miR-182)* embryos after microinjection of *cacnb4b/cacna2d1* mRNAs, compared to RFP as control. **d** Analysis of 72hpf Tbx5a or CT morphants in the *Tg(GAL4/sponge-miR-182)* background. For comparison wt AB and *Tg(myl7:GAL4)* transgenic lines were also analyzed. Statistics: Student's *t* test $*p<0.05$; $**p<0.01$; $***p<0.001$

downregulates myocardial proliferation as reported for Tbx5 [42]. Particularly interesting is the impact of miR-182 on cardiac function. HOS mice revealed conduction system defects with sporadic electrophysiological anomalies [8]. Potential miR-182 cardiac functions were further elucidated by an in silico analysis, which identified several calcium channel subunit genes involved in calcium homeostasis; these include the LTCC *Cacna2d1*, *Cacnb2*, *Cacnb4*, and *Cacng5* genes. Besides the four KEGG cardiac pathways which were investigated further (Fig. S12A), it is interesting

to note that other KEGG pathways which resulted enriched in putative miR-182 targets (Fig. S11), are known to affect calcium homeostasis and cardiac contractility. In particular, the Wnt signaling pathway [33] and PI3K-Akt, both considered master regulators of LTCC activity [35, 43], were enriched, as well as the calcium signaling KEGG itself. Modulation of other in silico identified targets cannot be excluded, and remain to be further studied. The decrease of *cacnb2.2*, *cacnb4b* and *cacna2d1* expression in isolated miR-182-OE hearts was confirmed by ddPCR quantification. In further studies of *cacna2d1,* data from in vitro luciferase assays support its regulation by miR-182 (Fig. S13A). We further note that a decrease of *cacna2d1* expression was detected in our cardiac *Tbx5*$^{del/+}$ mouse samples relative to wt samples (not shown). Others have reported a strong downregulation of *cacna2d2* in the HOS transcriptome analysis by Mori et al., [8]. We predict that the increase of miR-182 levels and consequent decrease of LTCC α2, δ and β subunits expression will produce changes in the amplitude and kinetics of calcium currents underlying myocyte action potential generation. Indeed, we have observed a bursting electrical activity combined with arrhythmias in some miR-182 microinjected hearts, while ECG recordings revealed alterations of ECG waves, indicating a fickle orientation of the atrial and ventricular mean electrical vectors (Fig. 4c).

Parallel recordings of atrial and ventricular mechanical events indicated that blockage could occur in either chamber (Fig. S13 C4). Since the atrium is the first chamber to be blocked, it is conceivable that defective membrane depolarization may affect both atrial and ventricular myocytes. Moreover, during each pause in the electrical activity an impaired relaxation occurs, suggesting that Ca^{2+} reticular uptake is poor. In fact, a slow falling phase of the calcium wave was found in experiments exploiting the *Tg(myl7:CaGFP)* line (Fig. S13D5, 6). These data were further supported by analysis of our zebrafish transgenic lines stably overexpressing or downregulating miR-182 in cardiomyocytes. The *Tg(GAL4/miR-182)* embryos show milder morphological defects compared with miR-182-OE embryos, in accord with the later and lower burst of this miRNA in transgenic embryos compared to miRNA mimic injected embryos. This observation indicates that the dysregulation of other Tbx5 effectors might contribute to create the stretched cardiac phenotype that resembles *hst* mutants [7]. It is important to appreciate that alteration of a single effector is not expected to recapitulate the complex phenotype caused by depletion of Tbx5, a transcription factor known to modulate hundreds of cardiac genes. Despite the mild morphological defects, 6 dpf *Tg(GAL4/miR-182)* embryos exhibited widespread alterations of rhythm (Fig. 5B2–3), and ECG analysis highlighted a 2:1 activity pattern, alternating between normal and attenuated P and R waveforms (Fig. 5B5). However, several reports demonstrate that the LTCC β subunits are also involved in many other processes such as cardiac cell proliferation and heart integrity [31, 44]. The observed alterations of physiological properties in both miR-182 microinjected and overexpressing transgenic embryos might be explained by abnormal calcium handling, due to reduced expression of both LTCC subunits and sarco/endoplasmic reticulum Ca^{2+}-ATPase (SERCA) pumps. Analysis of miR-182 targets confirmed the reduced expression of LTCC subunits but failed to detect changes in the expression of SERCA calcium pumps. However, altered Ca^{2+} entry caused by reduced conductance in myocytes might affect modulation of Ca^{2+} pumps, thereby modifying Ca^{2+}cycling. Therefore, we cannot exclude that the morphological alterations affecting hearts overexpressing miR-182 are partially due to altered channel subunits. The observation that injections of *cacnb4b* and *cacna2d1* transcripts are able to improve both cardiac rhythm and morphology in transient (Fig. 4d–f) or stable (Fig. 5c) miR-182-OE embryos provides strong support for the role of LTCC genes as miR-182 targets and their involvement in the prevalence of cardiac anomalies.

MiR-183 cluster members are up-regulated both in *Tbx5*$^{lox/+}$ and *Tbx5*$^{del/+}$hearts suggesting that a hypomorphic allele may contribute to the altered expression of these miRNAs, as previously observed by others [8]. Moreover, our transactivation studies (Fig. 1d) suggest that Tbx5 action might be mediated by Klf4. This observation is in line with RNA-seq [18] and ChIP-seq [45] data. Our data suggest that Klf4-mediated modulation of miR-182 might affect cardiac Ca^{2+}cycling.

The identification of miR-182 as a mediator of TBX5 activity prompted us to compare the functional consequences of miR-182 overexpression with the HOS phenotype. Some of the genes identified in silico as miR-182 targets are de-regulated in HOS patients and potentially related to other arrhythmic human syndromes as well [8, 46]. In mouse, *Tbx5* haploinsufficiency results in defects of ventricular relaxation. In fact, ventricular myocytes have impaired Ca^{2+} uptake dynamics and prolonged calcium transients with sporadic events of AV block, SA pauses and tachycardia [47, 48].

There are parallels between the functional consequences of miR-182 overexpression and HOS pathology, although the complexity of the entire system and the reciprocal interactions between morphology and physiology cannot allow a more precise alignment of the symptoms. In our study, the relationship between miR-182 and Tbx5 is strongly supported by the rescue experiments: downregulation of miR-182 halved the number of embryos with *heartstring* phenotypes, doubled the occurrence of wt phenotype in *tbx5* morphants, and rescued *heartstring tbx5* mutant embryos. Conversely, defects caused by Tbx5 depletion were significantly reduced in *Tg(GAL4/sponge-miR-182)* line stably

expressing a miR-182 antagonist in cardiomyocytes. It is noteworthy that miR-182 modulation failed to cause alterations in fin morphology, supporting the hypothesis that it is a cardiac-specific regulator of Tbx5 patterns. To further verify whether this microRNA might be a Tbx5 effector involved in other arrhythmic syndromes would be of clinical relevance and warrants further study. In support of this view, induced atrial fibrillation in pigs caused a marked downregulation of Tbx5 and upregulation of miR-182 [49]. Further investigations will help to assess whether miR-182 might act as a Tbx5 effector in large animal models of heart failure which arise from lethal arrhythmic events [50]. Our data will be helpful to design effective therapeutic approaches for clinical management of sudden death related to congenital heart disease.

Acknowledgements We are grateful to Dr.Elena Chiavacci (International Centre for Genetic Engineering and Biotechnology,Trieste, Italy) for experimental assistance, Dr. Marnie Halpern (Carnegie Institution Baltimore, Maryland) for kindly providing the pME-Galff-2a-mCherry and 4XNR UAS GFP plasmids, Dr. Héctor Sanchez Iranzo (Centro Nacional de Investigaciones Cardiovasculares Carlos III, 28029 Madrid,Spain) for kindly providing pDestCrysGFP plasmid and Prof. Sheng-Ping L. Hwang (Institute of Cellular and Organismic Biology Academia Sinica Taiwan) for the kind gift of the T7TS-klf4a plasmid for dre klf4 overexpression in zebrafish embryos. RF thanks Didier Stainier (Department of Developmental Genetics, Max Planck Institute for Heart and Lung Research, Bad Nauheim, Germany) for support.

Funding The project was supported by grants from the American Heart Association (17AIREA33660773) and PCOM Center for Chronic Disorders of Aging to C.J. Hatcher and by the American Heart Association 17GRNT33460256 to D.Garrity.

References

1. Bruneau BG, Logan M, Davis N, Levi T, Tabin CJ, Seidman JG, Seidman CE (1999) Chamber-specific cardiac expression of Tbx5 and heart defects in Holt-Oram syndrome. Dev Biol 211(1):100–108
2. Basson CT, Bachinsky DR, Lin RC, Levi T, Elkins JA, Soults J, Grayzel D, Kroumpouzou E, Traill TA, Leblanc-Straceski J, Renault B, Kucherlapati R, Seidman JG, Seidman CE (1997) Mutations in human TBX5 [corrected] cause limb and cardiac malformation in Holt-Oram syndrome. Nat Genet 15(1):30–35. https://doi.org/10.1038/ng0197-30
3. Christophersen IE, Rienstra M, Roselli C, Yin X, Geelhoed B, Barnard J, Lin H, Arking DE, Smith AV, Albert CM, Chaffin M, Tucker NR, Li M, Klarin D, Bihlmeyer NA, Low SK, Weeke PE, Muller-Nurasyid M, Smith JG, Brody JA, Niemeijer MN, Dorr M, Trompet S, Huffman J, Gustafsson S, Schurmann C, Kleber ME, Lyytikainen LP, Seppala I, Malik R, Horimoto A, Perez M, Sinisalo J, Aeschbacher S, Theriault S, Yao J, Radmanesh F, Weiss S, Teumer A, Choi SH, Weng LC, Clauss S, Deo R, Rader DJ, Shah SH, Sun A, Hopewell JC, Debette S, Chauhan G, Yang Q, Worrall BB, Pare G, Kamatani Y, Hagemeijer YP, Verweij N, Siland JE, Kubo M, Smith JD, Van Wagoner DR, Bis JC, Perz S, Psaty BM, Ridker PM, Magnani JW, Harris TB, Launer LJ, Shoemaker MB, Padmanabhan S, Haessler J, Bartz TM, Waldenberger M, Lichtner P, Arendt M, Krieger JE, Kahonen M, Risch L, Mansur AJ, Peters A, Smith BH, Lind L, Scott SA, Lu Y, Bottinger EB, Hernesniemi J, Lindgren CM, Wong JA, Huang J, Eskola M, Morris AP, Ford I, Reiner AP, Delgado G, Chen LY, Chen YI, Sandhu RK, Boerwinkle E, Eisele L, Lannfelt L, Rost N, Anderson CD, Taylor KD, Campbell A, Magnusson PK, Porteous D, Hocking LJ, Vlachopoulou E, Pedersen NL, Nikus K, Orho-Melander M, Hamsten A, Heeringa J, Denny JC, Kriebel J, Darbar D, Newton-Cheh C, Shaffer C, Macfarlane PW, Heilmann-Heimbach S, Almgren P, Huang PL, Sotoodehnia N, Soliman EZ, Uitterlinden AG, Hofman A, Franco OH, Volker U, Jockel KH, Sinner MF, Lin HJ, Guo X, Dichgans M, Ingelsson E, Kooperberg C, Melander O, Loos RJF, Laurikka J, Conen D, Rosand J, van der Harst P, Lokki ML, Kathiresan S, Pereira A, Jukema JW, Hayward C, Rotter JI, Marz W, Lehtimaki T, Stricker BH, Chung MK, Felix SB, Gudnason V, Alonso A, Roden DM, Kaab S, Chasman DI, Heckbert SR, Benjamin EJ, Tanaka T, Lunetta KL, Lubitz SA, Ellinor PT (2017) Large-scale analyses of common and rare variants identify 12 new loci associated with atrial fibrillation. Nat Genet 49(6):946–952. https://doi.org/10.1038/ng.3843
4. Ma JF, Yang F, Mahida SN, Zhao L, Chen X, Zhang ML, Sun Z, Yao Y, Zhang YX, Zheng GY, Dong J, Feng MJ, Zhang R, Sun J, Li S, Wang QS, Cao H, Benjamin EJ, Ellinor PT, Li YG, Tian XL (2016) TBX5 mutations contribute to early-onset atrial fibrillation in Chinese and caucasians. Cardiovasc Res 109(3):442–450. https://doi.org/10.1093/cvr/cvw003
5. Bruneau BG, Nemer G, Schmitt JP, Charron F, Robitaille L, Caron S, Conner DA, Gessler M, Nemer M, Seidman CE, Seidman JG (2001) A murine model of Holt-Oram syndrome defines roles of the T-box transcription factor Tbx5 in cardiogenesis and disease. Cell 106(6):709–721
6. Nadadur RD, Broman MT, Boukens B, Mazurek SR, Yang X, van den Boogaard M, Bekeny J, Gadek M, Ward T, Zhang M, Qiao Y, Martin JF, Seidman CE, Seidman J, Christoffels V, Efimov IR, McNally EM, Weber CR, Moskowitz IP (2016) Pitx2 modulates a Tbx5-dependent gene regulatory network to maintain atrial rhythm. Sci Transl Med 8(354):354
7. Garrity DM, Childs S, Fishman MC (2002) The heartstrings mutation in zebrafish causes heart/fin Tbx5 deficiency syndrome. Development 129(19):4635–4645
8. Mori AD, Zhu Y, Vahora I, Nieman B, Koshiba-Takeuchi K, Davidson L, Pizard A, Seidman JG, Seidman CE, Chen XJ, Henkelman RM, Bruneau BG (2006) Tbx5-dependent rheostatic control of cardiac gene expression and morphogenesis. Dev Biol 297(2):566–586
9. D'Aurizio R, Russo F, Chiavacci E, Baumgart M, Groth M, D'Onofrio M, Arisi I, Rainaldi G, Pitto L, Pellegrini M (2016) Discovering miRNA regulatory networks in Holt-Oram syndrome using a zebrafish model. Front Bioeng Biotechnol 4:60. https://doi.org/10.3389/fbioe.2016.00060
10. Chiavacci E, D'Aurizio R, Guzzolino E, Russo F, Baumgart M, Groth M, Mariani L, D'Onofrio M, Arisi I, Pellegrini M, Cellerino A, Cremisi F, Pitto L (2015) MicroRNA 19a replacement partially rescues fin and cardiac defects in zebrafish model of Holt Oram syndrome. Sci Rep 5:18240. https://doi.org/10.1038/srep18240
11. Chiavacci E, Dolfi L, Verduci L, Meghini F, Gestri G, Evangelista AMM, Wilson SW, Cremisi F, Pitto L (2012) MicroRNA 218 mediates the effects of tbx5a over-expression on zebrafish heart development. PLoS One 7 (11). doi:ARTN e50536 https://doi.org/10.1371/journal.pone.0050536
12. Guzzolino E, Chiavacci E, Ahuja N, Mariani L, Evangelista M, Ippolito C, Rizzo M, Garrity D, Cremisi F, Pitto L (2018) Post-transcriptional Modulation of Sphingosine-1-Phosphate Receptor 1 by miR-19a Affects Cardiovascular Development in Zebrafish. Front Cell Dev Biol. 6:58. https://doi.org/10.3389/fcell.2018.00058

13. Sakai K, Miyazaki J (1997) A transgenic mouse line that retains Cre recombinase activity in mature oocytes irrespective of the cre transgene transmission. Biochem Biophys Res Commun 237(2):318–324
14. Baumgart M, Groth M, Priebe S, Appelt J, Guthke R, Platzer M, Cellerino A (2012) Age-dependent regulation of tumor-related microRNAs in the brain of the annual fish *Nothobranchius furzeri*. Mech Ageing Dev 133(5):226–233. https://doi.org/10.1016/j.mad.2012.03.015
15. Anders S, Huber W (2010) Differential expression analysis for sequence count data. Genome Biol 11(10):R106. https://doi.org/10.1186/gb-2010-11-10-r106
16. Chi NC, Shaw RM, Jungblut B, Huisken J, Ferrer T, Arnaout R, Scott I, Beis D, Xiao T, Baier H, Jan LY, Tristani-Firouzi M, Stainier DY (2008) Genetic and physiologic dissection of the vertebrate cardiac conduction system. PLoS Biol 6(5):e109
17. Umemoto N, Nishimura Y, Shimada Y, Yamanaka Y, Kishi S, Ito S, Okamori K, Nakamura Y, Kuroyanagi J, Zhang Z, Zang L, Wang Z, Nishimura N, Tanaka T (2013) Fluorescent-based methods for gene knockdown and functional cardiac imaging in zebrafish. Mol Biotechnol 55(2):131–142. https://doi.org/10.1007/s12033-013-9664-6
18. Waldron L, Steimle JD, Greco TM, Gomez NC, Dorr KM, Kweon J, Temple B, Yang XH, Wilczewski CM, Davis IJ, Cristea IM, Moskowitz IP, Conlon FL (2016) The cardiac TBX5 interactome reveals a chromatin remodeling network essential for cardiac septation. Dev Cell 36(3):262–275. https://doi.org/10.1016/j.devcel.2016.01.009
19. Segura MF, Jubierre L, Li S, Soriano A, Koetz L, Gaziel-Sovran A, Masanas M, Kleffman K, Dankert JF, Walsh MJ, Hernando E (2017) Kruppel-like factor 4 (KLF4) regulates the miR-183 ~ 96–182 cluster under physiologic and pathologic conditions. Oncotarget 8(16):26298–26311. https://doi.org/10.18632/oncotarget.15459
20. Yang KC, Yamada KA, Patel AY, Topkara VK, George I, Cheema FH, Ewald GA, Mann DL, Nerbonne JM (2014) Deep RNA sequencing reveals dynamic regulation of myocardial noncoding RNAs in failing human heart and remodeling with mechanical circulatory support. Circulation 129(9):1009–1021. https://doi.org/10.1161/circulationaha.113.003863
21. Cakmak HA, Coskunpinar E, Ikitimur B, Barman HA, Karadag B, Tiryakioglu NO, Kahraman K, Vural VA (2015) The prognostic value of circulating microRNAs in heart failure: preliminary results from a genome-wide expression study. J Cardiovasc Med (Hagerstown) 16(6):431–437. https://doi.org/10.2459/jcm.0000000000000233
22. Li N, Hwangbo C, Jaba IM, Zhang J, Papangeli I, Han J, Mikush N, Larrivee B, Eichmann A, Chun HJ, Young LH, Tirziu D (2016) miR-182 modulates myocardial hypertrophic response induced by angiogenesis in heart. Sci Rep 6:21228. https://doi.org/10.1038/srep21228
23. Kuppusamy KT, Jones DC, Sperber H, Madan A, Fischer KA, Rodriguez ML, Pabon L, Zhu WZ, Tulloch NL, Yang X, Sniadecki NJ, Laflamme MA, Ruzzo WL, Murry CE, Ruohola-Baker H (2015) Let-7 family of microRNA is required for maturation and adult-like metabolism in stem cell-derived cardiomyocytes. Proc Natl Acad Sci USA 112(21):E2785–2794. https://doi.org/10.1073/pnas.1424042112
24. Bakkers J (2011) Zebrafish as a model to study cardiac development and human cardiac disease. Cardiovasc Res 91(2):279–288. https://doi.org/10.1093/cvr/cvr098
25. Huang CJ, Tu CT, Hsiao CD, Hsieh FJ, Tsai HJ (2003) Germline transmission of a myocardium-specific GFP transgene reveals critical regulatory elements in the cardiac myosin light chain 2 promoter of zebrafish. Dev Dyn 228(1):30–40. https://doi.org/10.1002/dvdy.10356
26. Auman HJ, Coleman H, Riley HE, Olale F, Tsai HJ, Yelon D (2007) Functional modulation of cardiac form through regionally confined cell shape changes. PLoS Biol 5(3):e53. https://doi.org/10.1371/journal.pbio.0050053
27. Yelon D (2001) Cardiac patterning and morphogenesis in zebrafish. Dev Dyn 222(4):552–563. https://doi.org/10.1002/dvdy.1243
28. Georges R, Nemer G, Morin M, Lefebvre C, Nemer M (2008) Distinct expression and function of alternatively spliced Tbx5 isoforms in cell growth and differentiation. Mol Cell Biol 28(12):4052–4067. https://doi.org/10.1128/mcb.02100-07
29. Hiroi Y, Kudoh S, Monzen K, Ikeda Y, Yazaki Y, Nagai R, Komuro I (2001) Tbx5 associates with Nkx2-5 and synergistically promotes cardiomyocyte differentiation. Nat Genet 28(3):276–280. https://doi.org/10.1038/90123
30. Parrie LE, Renfrew EM, Wal AV, Mueller RL, Garrity DM (2013) Zebrafish tbx5 paralogs demonstrate independent essential requirements in cardiac and pectoral fin development. Dev Dyn 242(5):485–502. https://doi.org/10.1002/dvdy.23953
31. Chernyavskaya Y, Ebert AM, Milligan E, Garrity DM (2012) Voltage-gated calcium channel CACNB2 (beta2.1) protein is required in the heart for control of cell proliferation and heart tube integrity. Dev Dyn 241(4):648–662. https://doi.org/10.1002/dvdy.23746
32. Nielsen BS, Moller T, Holmstrom K (2012) Combined MicroRNA in situ hybridization and immunohistochemical detection of protein markers. Eur J Cancer 48:S216–S216. https://doi.org/10.1016/s0959-8049(12)71524-1
33. Lorenzon A, Calore M, Poloni G, De Windt LJ, Braghetta P, Rampazzo A (2017) Wnt/beta-catenin pathway in arrhythmogenic cardiomyopathy. Oncotarget 8(36):60640–60655. https://doi.org/10.18632/oncotarget.17457
34. Cohen ED, Tian Y, Morrisey EE (2008) Wnt signaling: an essential regulator of cardiovascular differentiation, morphogenesis and progenitor self-renewal. Development 135(5):789–798. https://doi.org/10.1242/dev.016865
35. Ghigo A, Laffargue M, Li M, Hirsch E (2017) PI3K and calcium signaling in cardiovascular disease. Circ Res 121(3):282–292. https://doi.org/10.1161/circresaha.117.310183
36. Sciarretta S, Forte M, Frati G, Sadoshima J (2018) New insights into the role of mTOR signaling in the cardiovascular system. Circ Res 122(3):489–505. https://doi.org/10.1161/circresaha.117.311147
37. Ehler E (2018) Actin-associated proteins and cardiomyopathy-the 'unknown' beyond troponin and tropomyosin. Biophys Rev 10(4):1121–1128. https://doi.org/10.1007/s12551-018-0428-1
38. Landstrom AP, Dobrev D, Wehrens XHT (2017) Calcium signaling and cardiac arrhythmias. Circ Res 120(12):1969–1993. https://doi.org/10.1161/circresaha.117.310083
39. Bennett JS, Stroud DM, Becker JR, Roden DM (2013) Proliferation of embryonic cardiomyocytes in zebrafish requires the sodium channel scn5Lab. Genesis 51(8):562–574. https://doi.org/10.1002/dvg.22400
40. Cassis P, Cerullo D, Zanchi C, Corna D, Lionetti V, Giordano F, Novelli R, Conti S, Casieri V, Matteucci M, Locatelli M, Taraboletti G, Villa S, Gastoldi S, Remuzzi G, Benigni A, Zoja C (2018) ADAMTS13 deficiency shortens the life span of mice with experimental diabetes. Diabetes 67(10):2069–2083. https://doi.org/10.2337/db17-1508
41. Sehnert AJ, Stainier DY (2002) A window to the heart: can zebrafish mutants help us understand heart disease in humans? Trends Genet 18(10):491–494
42. Goetz SC, Brown DD, Conlon FL (2006) TBX5 is required for embryonic cardiac cell cycle progression. Development 133(13):2575–2584

43. Sun H, Kerfant BG, Zhao D, Trivieri MG, Oudit GY, Penninger JM, Backx PH (2006) Insulin-like growth factor-1 and PTEN deletion enhance cardiac L-type Ca2 + currents via increased PI3Kalpha/PKB signaling. Circ Res 98(11):1390–1397
44. Subramanyam P, Obermair GJ, Baumgartner S, Gebhart M, Striessnig J, Kaufmann WA, Geley S, Flucher BE (2009) Activity and calcium regulate nuclear targeting of the calcium channel beta4b subunit in nerve and muscle cells. Channels (Austin) 3(5):343–355. https://doi.org/10.4161/chan.3.5.9696
45. He J, Yang D, Wang C, Liu W, Liao J, Xu T, Bai C, Chen J, Lin K, Huang C, Dong Q (2011) Chronic zebrafish low dose decabrominated diphenyl ether (BDE-209) exposure affected parental gonad development and locomotion in F1 offspring. Ecotoxicology 20(8):1813–1822. https://doi.org/10.1007/s10646-011-0720-3
46. Burashnikov E, Pfeiffer R, Barajas-Martinez H, Delpon E, Hu D, Desai M, Borggrefe M, Haissaguerre M, Kanter R, Pollevick GD, Guerchicoff A, Laino R, Marieb M, Nademanee K, Nam GB, Robles R, Schimpf R, Stapleton DD, Viskin S, Winters S, Wolpert C, Zimmern S, Veltmann C, Antzelevitch C (2010) Mutations in the cardiac L-type calcium channel associated with inherited J-wave syndromes and sudden cardiac death. Heart Rhythm 7(12):1872–1882. https://doi.org/10.1016/j.hrthm.2010.08.026
47. Arnolds DE, Liu F, Fahrenbach JP, Kim GH, Schillinger KJ, Smemo S, McNally EM, Nobrega MA, Patel VV, Moskowitz IP (2012) TBX5 drives Scn5a expression to regulate cardiac conduction system function. J Clin Invest 122(7):2509–2518
48. Zhu Y, Gramolini AO, Walsh MA, Zhou YQ, Slorach C, Friedberg MK, Takeuchi JK, Sun H, Henkelman RM, Backx PH, Redington AN, Maclennan DH, Bruneau BG (2008) Tbx5-dependent pathway regulating diastolic function in congenital heart disease. Proc Natl Acad Sci USA 105(14):5519–5524. https://doi.org/10.1073/pnas.0801779105
49. Torrado M, Franco D, Lozano-Velasco E, Hernandez-Torres F, Calvino R, Aldama G, Centeno A, Castro-Beiras A, Mikhailov A (2015) A MicroRNA-transcription factor blueprint for early atrial arrhythmogenic remodeling. Biomed Res Int 2015:263151. https://doi.org/10.1155/2015/263151
50. Hegyi B, Bossuyt J, Griffiths LG, Shimkunas R, Coulibaly Z, Jian Z, Grimsrud KN, Sondergaard CS, Ginsburg KS, Chiamvimonvat N, Belardinelli L, Varro A, Papp JG, Pollesello P, Levijoki J, Izu LT, Boyd WD, Banyasz T, Bers DM, Chen-Izu Y (2018) Complex electrophysiological remodeling in postinfarction ischemic heart failure. Proc Natl Acad Sci USA 115(13):E3036–E3044. https://doi.org/10.1073/pnas.1718211115

Publisher's Note Springer Nature remains neutral with regard to jurisdictional claims in published maps and institutional affiliations.